

**Original citation:**

Hu, Xiao-Bing, Wang, Ming, Ye, Qian, Han, Zhangan and Leeson, Mark S., 1963-. (2014) Multi-objective new product development by complete Pareto front and ripple-spreading algorithm. *Neurocomputing*, Volume 142 . pp. 4-15.

**Permanent WRAP url:**

<http://wrap.warwick.ac.uk/63879>

**Copyright and reuse:**

The Warwick Research Archive Portal (WRAP) makes this work of researchers of the University of Warwick available open access under the following conditions. Copyright © and all moral rights to the version of the paper presented here belong to the individual author(s) and/or other copyright owners. To the extent reasonable and practicable the material made available in WRAP has been checked for eligibility before being made available.

Copies of full items can be used for personal research or study, educational, or not-for-profit purposes without prior permission or charge. Provided that the authors, title and full bibliographic details are credited, a hyperlink and/or URL is given for the original metadata page and the content is not changed in any way.

**Publisher statement:**

NOTICE: this is the author's version of a work that was accepted for publication in *Neurocomputing*. The changes resulting from the publishing process, such as peer review, editing, corrections, structural formatting, and other quality control mechanisms may not be reflected in this document. Changes may have been made to this work since it was submitted for publication. A definitive version was subsequently published in <http://dx.doi.org/10.1016/j.neucom.2014.02.058>

**A note on versions:**

The version presented here may differ from the published version or, version of record, if you wish to cite this item you are advised to consult the publisher's version. Please see the 'permanent WRAP url' above for details on accessing the published version and note that access may require a subscription.

For more information, please contact the WRAP Team at: [publications@warwick.ac.uk](mailto:publications@warwick.ac.uk)



<http://wrap.warwick.ac.uk/>

# **Multi-Objective New Product Development by Complete Pareto Front and Ripple-Spreading Algorithm\***

Xiao-Bing Hu<sup>1,3</sup>, Ming Wang<sup>1</sup>, Qian Ye<sup>1</sup>, Zhangang Han<sup>2</sup>, and Mark S. Leeson<sup>3</sup>

<sup>1</sup> State Key Laboratory of Earth Surface Processes and Resource Ecology,  
Beijing Normal University, China.

<sup>2</sup> School of Systems Science, Beijing Normal University, China.

<sup>3</sup> School of Engineering, University of Warwick, Coventry, UK.

\* This work was supported in part by the China “973” Project under Grant 2012CB955404, the project grant 2012-TDZY-21 from Beijing Normal University, China, and the Seventh Framework Programme (FP7) of the European Union under Grant PIOF-GA-2011-299725.

## **Abstract**

Given several different new product development projects and limited resources, this paper is concerned with the optimal allocation of resources among the projects. This is clearly a multi-objective optimization problem (MOOP), because each new product development project has both a profit expectation and a loss expectation, and such expectations vary according to allocated resources. In such a case, the goal of multi-objective new product development (MONPD) is to maximize the profit expectation while minimizing the loss expectation. As is well known, Pareto optimality and the Pareto front are extremely important to resolve MOOPs. Unlike many other MOOP methods which provide only a single Pareto optimal solution or an approximation of the Pareto front, this paper reports a novel method to calculate the complete Pareto front for the MONPD. Some theoretical conditions and a ripple-spreading algorithm together play a crucial role in finding the complete Pareto front for the MONPD. Simulation results illustrate that the reported method, by calculating the complete Pareto front, can provide the best support to decision makers in the MONPD.

**Key words:** Multi-Objective Optimization, New Product Development, Pareto Front, Ripple-Spreading Algorithm.

## **1 INTRODUCTION**

New product development plays an extremely crucial role in company survival and success in the modern increasingly competitive global market; every year, billions of dollars are invested in various new product development projects (NPDPs) worldwide [1]-[5]. Obviously, not all NPDPs are successful, and there never lack examples where a big-brand company collapses after an NPDP because it misjudges market trends and/or consumes considerable of capital. To avoid such a tragedy, an effective practice is "not to put all eggs in one basket". Therefore, a company may often have several NPDPs proceeding at one time. Each NPDP has both a profit expectation and a loss expectation, and such expectations vary according to the resources allocated to the NPDP. Basically, the greater the allocated resources the higher the profit expectation is. Increased allocated resources may reduce the failure possibility during the development stage of an NPDP, but cannot necessarily provide a better guarantee of market success. If anything goes wrong during the marketing stage due to many external, uncertain and uncontrollable factors, the larger resource allocation only means a bigger loss. Common sense in the financial sector predicts that a high profit expectation usually comes with a big loss expectation [6]. Therefore, decision makers often

have to make a choice between high-profit-big-risk options and low-profit-small-risk options, based on their risk taking willingness and understanding of a market environment. Since available resources are always limited, decision makers usually need to optimize their investment portfolio, in order to maximize the profit expectation while minimizing the loss expectation – two conflicting objectives. In this paper, we are particularly concerned with the problem of allocating limited resources among several NPDPs, so that the overall profit expectation can be maximized while the overall loss expectation can be minimized. This clearly fits in the scope of a multi-objective optimization problem (MOOP), and hereafter we call the concerned problem *multi-objective new product development* (MONPD).

To resolve the MONPD, we need to make use of the Pareto front. As the most important concept in MOOPs, the Pareto front originates from the concept of Pareto efficiency proposed to study economic efficiency and income distribution [7]. In general MOOPs, a solution is called Pareto optimal if there exists no other solution that is better in terms of at least one objective and is not worse in terms of all other objectives [8] [9]. The projection of a Pareto optimal solution in the objective space is called a Pareto point. All Pareto points, i.e., the projections of all Pareto optimal solutions, compose the complete Pareto front of an MOOP.

The history of such problems is long resulting in the development of many methods for resolving various MOOPs. Basically, most methods can be classified into three categories: aggregate objective function (AOF) based methods [10]-[14], Pareto-compliant ranking (PCR) based methods [15]-[25], and constrained objective (COF) function based methods [26]-[30]. An AOF method combines all of the objectives of an MOOP to construct a single aggregate objective function, and then resolve the single-objective problem to get a Pareto optimal solution. However, it involves subjectiveness in constructing an AOF, and it often fails to find some Pareto optimal solutions if the Pareto front is not convex. A PCR method may overcome such drawbacks of AOF methods by operating on a pool of candidate solutions and favoring non-dominated solutions. Population-based evolutionary approaches (such as genetic algorithms, particle swarm optimization and ant colony optimization) often play a key role in PCR methods to identify multiple Pareto optimal candidate solutions. It should be noted that, due to the stochastic nature of PCR methods, their outputs are Pareto optimal candidate solutions, not necessarily real Pareto optimal solutions. Theoretically, COF methods, by optimizing only one single objective while treating all other objectives as extra constraints, may avoid both the subjectiveness of AOF methods and the loss of Pareto optimality in PCR methods.

Calculating complete Pareto front is a relatively less discussed topic in the study of MOOPs. Theoretically, some nonlinear AOF based methods can prove that for any Pareto point on the Pareto front

a set of AOF coefficients definitely exists which can lead to that Pareto point. However, the difficulty is that there is a lack of a practicable method to find those sets of coefficients that will help to identify the complete Pareto front [28]. For PCR methods, guaranteeing the complete Pareto front is theoretically a mission impossible, largely because of the stochastic nature of employed population-based approaches [15]. COF methods, given well posed objective function constraints, may theoretically guarantee the finding of the complete Pareto front but like AOF methods, how the practicality of finding proper constraints is a big issue [30]. Therefore, most existing methods can only produce an incomplete or approximate Pareto front [10], [15], [26]-[30]. In particular, as pointed out in [26], very few results are available on the quality of the approximation of the Pareto front for discrete MOOPs.

We have recently proposed a deterministic method which can, theoretically and practically, guarantee the finding of complete Pareto front for discrete MOOPs [31]. Some theoretical conditions and a general methodology were reported in [31], and a case study on a multi-objective route optimization problem (ROP) was used to prove the correctness and practicability. In this paper, we will particularly apply the method of [31] to the MONPD. Actually, there is a substantial body of literature on optimizing investment portfolios [6], [32]-[38] similar to MONPD, but little work has been reported to calculate complete Pareto front of such investment portfolio optimization problems. To calculate the complete Pareto front for MONPD, firstly, we will improve the theoretical conditions and the methodology reported in [31]. The most challenging part in the method of [31] is to design an algorithm that is capable of finding the global  $k^{\text{th}}$  best solution for any given  $k$  in terms of a given single objective. Designing such an algorithm is largely problem-dependent, and is often difficult because most optimization algorithms only calculate the global 1<sup>st</sup> best solution. MONPD is quite different from the ROP in [31]. For example, in the ROP, every objective needs to be minimized; however, in MONPD, the profit expectation needs to be maximized although the loss expectation is to be minimized. Therefore, MONPD demands a new algorithm to calculate the general  $k^{\text{th}}$  best (rather than only the  $k^{\text{th}}$  smallest) single-objective solution. By successfully developing a new ripple-spreading algorithm for MONPD, this paper will further prove the practicability and the potential of the methodology of resolving discrete MOOPs by calculating complete Pareto front.

The remainder of this paper is organized as following. Section 2 gives some theoretical results for calculating complete Pareto front for discrete MOOPs. Section 3 describes mathematically the details of MONPD. Section 4 reports a ripple-spreading algorithm for MONPD. Simulation results are given in Section 5, and the paper ends with some conclusions and discussions on future work in Section 5.

## 2 THEORETICAL RESULTS FOR CALCULATING THE COMPLETE PARETO FRONT

We have recently reported some theoretical results and a general methodology to guarantee, theoretically and practicably, the finding of the complete Pareto front for discrete MOOPs [31]. The work in [31] is the theoretical foundation of this application paper. In this section, we will introduce some improvements to the work of [31], in order to better apply to MONPD later.

First of all, we need a general mathematical formulation of discrete MOOPs as following:

$$\min_x [g_1(x), g_2(x), \dots, g_{N_{Obj}}(x)]^T, \quad (1)$$

subject to

$$h_I(x) \leq 0, \quad (2)$$

$$h_E(x) = 0, \quad (3)$$

$$x \in \Omega_X, \quad (4)$$

where  $g_i$  is the  $i$ th objective function of the total  $N_{Obj}$  objective functions,  $h_I$  and  $h_E$  are the inequality and equality constraints, respectively,  $x$  is the vector of optimization or decision variables belonging to the set of  $\Omega_X$ , and  $x$  is of discrete value. A Pareto-optimal solution  $x^*$  to the above problem is so that there exists no  $x$  that makes

$$g_i(x) \leq g_i(x^*), \text{ for all } i=1, \dots, N_{Obj}, \quad (5)$$

$$g_j(x) < g_j(x^*), \text{ for at least one } j \in [1, \dots, N_{Obj}]. \quad (6)$$

The projection of such an  $x^*$  in the objective space is called a Pareto point. The above problem usually has a set of Pareto optimal solutions, whose projections compose the complete Pareto front.

### 2.1 Theoretical conditions

According to the theoretical results in [31], we have the following statements for discrete MOOPs.

**Lemma 1:** Suppose we sort all discrete  $x \in \Omega_X$  according to a certain objective function  $g_j(x)$ , and  $x_{j,i}$  has the  $i$ th smallest  $g_j$ . For a given constant  $c$ , if there exists an index  $k$  that satisfies

$$g_j(x_{j,k}) \leq c < g_j(x_{j,k+1}), \quad (7)$$

Then the number of Pareto points whose  $g_j \leq c$  is no more than  $k$ , and all the associated  $x$  values are included in the set  $[x_{j,1}, \dots, x_{j,k}]$ .

**Lemma 2:** Suppose we have a constant vector  $[c_1, \dots, c_{N_{Obj}}]$ , the element  $c_j$  is for objective function  $g_j$ , and after sorting all discrete  $x \in \Omega_X$  according to each objective function  $g_j$ , we have  $k_j$  satisfying Condition (7). If for any  $j=1, \dots, N_{Obj}$ ,

$$g_i(x_{j,k_j}) \leq g_i(x_{i,k_i}), \text{ for all } i \neq j, \quad (8)$$

then the total number of Pareto points is no more than

$$N_{PP} \leq \sum_{j=1}^{N_{Obj}} k_j, \quad (9)$$

and all associated  $x$  values are included in the union set

$$\Omega_{U1} = \bigcup_{j=1}^{N_{Obj}} [x_{j,1}, \dots, x_{j,k_j}], \quad j=1, \dots, N_{Obj}. \quad (10)$$

For more details about Lemma 1 and Lemma 2, one may refer to [31]. Based on Lemma 1 and Lemma 2, [31] reported a methodology which employs an iteration process to calculate the  $k_j$  best solutions in terms of objective function  $g_j$ , for all  $j=1, \dots, N_{Obj}$ . In the iteration process,  $k_j$  is increased step by step for all  $j=1, \dots, N_{Obj}$ , until a set of  $[k_1, \dots, k_{N_{Obj}}]$  is found to make Condition (8) hold.

In this paper, we give an upper bound for  $k_j$  (or upper bound for  $c_j$ ),  $j=1, \dots, N_{Obj}$ , in order to improve the computational efficiency of the methodology in [31]. To this end, we need the following new theorems.

**Theorem 1:** Suppose there exist  $x_1, \dots, x_{N_{Obj}}$  such that for any  $j \in [1, \dots, N_{Obj}]$ ,

$$g_i(x_j) \leq g_i(x_i), \text{ for all } i=1, \dots, N_{Obj}. \quad (11)$$

Then all Pareto-optimal solutions are included in the union set

$$\Omega_{U2} = \bigcup_{i=1}^{N_{Obj}} \{x : g_i(x) \leq g_i(x_i)\}. \quad (12)$$

**Proof:** Assume Theorem 1 is false. Therefore, there exists at least one Pareto-optimal solution, say  $x^*$ , that does not belong to the union set  $\Omega_{U2}$ , which means, according to the definition of  $\Omega_{U2}$  in Eq.(8), we have  $g_i(x_i) < g_i(x^*)$  for all  $i=1, \dots, N_{Obj}$ . Then for any  $j \in [1, \dots, N_{Obj}]$ , we have

$$g_i(x_j) \leq g_i(x_i) < g_i(x^*), \text{ for all } i=1, \dots, N_{Obj}. \quad (13)$$

This means  $x_1, \dots, x_{N_{Obj}}$  are all more Pareto efficient than  $x^*$ . In other words,  $x^*$  is not a Pareto-optimal solution at all. Therefore, the assumption must be false, and Theorem 1 must be true.

**Corollary 1:** Obviously, the set of the first best single-objective solutions  $[x_{1,1}, \dots, x_{N_{Obj},1}]$  satisfies Condition (11) in Theorem 1. Therefore, all Pareto-optimal solutions are included in the union set

$$\Omega_{U3} = \bigcup_{i=1}^{N_{Obj}} \{x : g_i(x) \leq g_i(x_{i,1})\}. \quad (14)$$

With the union set defined by Eq.(14), we have

**Theorem 2:** The constant vector  $[c_1, \dots, c_{N_{Obj}}]$  in Lemma 2 has an upper bound defined by

$$\bar{c}_j = \max_{i=1, \dots, N_{Obj}} g_j(x_{i,1}), \quad j=1, \dots, N_{Obj}. \quad (15)$$

Suppose the  $\bar{c}_j$  in Eq.(15) is the  $(\bar{k}_j)^{\text{th}}$  best solution in terms of  $g_j$ , then  $\bar{k}_j$  can be used as an upper bound

for  $k_j$  in Lemma 2,  $j=1, \dots, N_{Obj}$ .

Proof: Assume Theorem 2 is false, i.e., for at least a  $j \in [1, \dots, N_{Obj}]$ , there exists no  $c_j \leq \bar{c}_j$  that can make Condition (8) hold. This means that the complete Pareto front is not covered by the union set  $\Omega_{U1}$ , in other words, there exists at least one Pareto-optimal solution  $x^*$  that has  $\bar{c}_j < g_j(x^*)$ . Then according to Eq.(14) and Eq.(15), one has that this  $x^*$  is not included in the union set  $\Omega_{U3}$ , which is obviously against Corollary 1. Therefore, Theorem 2 must be true.

## 2.2 General methodology

In this sub-section, based on Theorem 1 and Theorem 2, we will modify the methodology reported in [31], in order to improve the computational efficiency. The modified general methodology to calculate the complete Pareto front for discrete MOOPs is described as following:

Step 1. Design a problem-dependent deterministic algorithm that is capable of calculating any global  $k^{\text{th}}$  best solution in terms of a single objective function  $g_j$ , for any  $j=1, \dots, N_{Obj}$ .

Step 2. Calculate the set of the first best single-objective solutions  $[x_{1,1}, \dots, x_{N_{Obj},1}]$ , and then determine the upper bound set  $[\bar{c}_1, \dots, \bar{c}_{N_{Obj}}]$  according to Eq.(15).

Step 3. Initialize  $k_j=1$ , for every  $j=1, \dots, N_{Obj}$ . Initialize the Pareto front associated  $x$  value set as  $\Omega_{PFx} = \emptyset$ . Calculate the  $(k_j+1)$ th global best solutions in terms of the single objective function  $g_j$ , i.e., calculate  $x_{j,k_j+1}$ , for every  $j=1, \dots, N_{Obj}$ .

Step 4. If for every  $j=1, \dots, N_{Obj}$ ,

$$g_j(x_{j,k_j}) < g_j(x_{j,k_j+1}), \quad (16)$$

$$g_i(x_{j,k_j}) \leq g_i(x_{i,k_i}), \text{ for all } i \neq j, \quad (17)$$

then go to Step 6. Otherwise, fix  $k_j$  for any  $j$  that has Conditions (16) and (17) both satisfied or has  $g_j(x_{j,k_j}) \geq \bar{c}_j$ , and increase  $k_j$  by one, i.e.,  $k_j=k_j+1$ , for the  $j$  that has Condition (16) satisfied for the most  $i$  values.

Step 5. For the newly increased  $k_j$ , calculate the  $(k_j+1)$ th global best solutions in terms of  $g_j$ , i.e., update  $x_{j,k_j+1}$ . Go to Step 4.

Step 6. Calculate the union set of  $[x_{j,1}, \dots, x_{j,k_j}]$ ,  $j=1, \dots, N_{Obj}$ , denoting as  $\Omega_{UX}$ .

Step 7. For any  $x \in \Omega_{UX}$ , if there exist no  $\tilde{x} \in \Omega_{UX}$  such that  $g_i(\tilde{x}) \leq g_i(x)$ , for all  $i=1, \dots, N_{Obj}$ , and  $g_j(\tilde{x}) < g_j(x)$ , for at least one  $j \in [1, \dots, N_{Obj}]$ , then we know the point  $[g_1, \dots, g_{N_{Obj}}]$  is a Pareto point.

Therefore, add  $x$  into  $\Omega_{PFx}$ , i.e.,  $\Omega_{PFx} = \Omega_{PFx} + \{x\}$ .

The basic methodology in [31] needs to keep calculating the  $k$  best solutions in terms of each single-objective function in the iteration process, whilst the modified methodology only calculates the  $k^{\text{th}}$  best single-objective solution in Step 2, Step 3 and Step 5. Another improvement in the modified methodology is the introduction of upper bound  $\bar{c}_j$  in Step 4, which avoids unnecessary operation of increasing any  $k_j$  with  $g_j(x_{j,k_j}) \geq \bar{c}_j$ . These modifications may obviously improve the computational efficiency to find the complete Pareto front for a discrete MOOP.

### 3 A MATHEMATICAL FORMULATION OF MONPD

Basically, MONPD is to allocate limited resources among several different new product development project (NPDPs), in order to maximize the profit expectation and minimize the loss expectation. Here we give a mathematical description of the MONPD as following, which is illustrated by Fig.1.

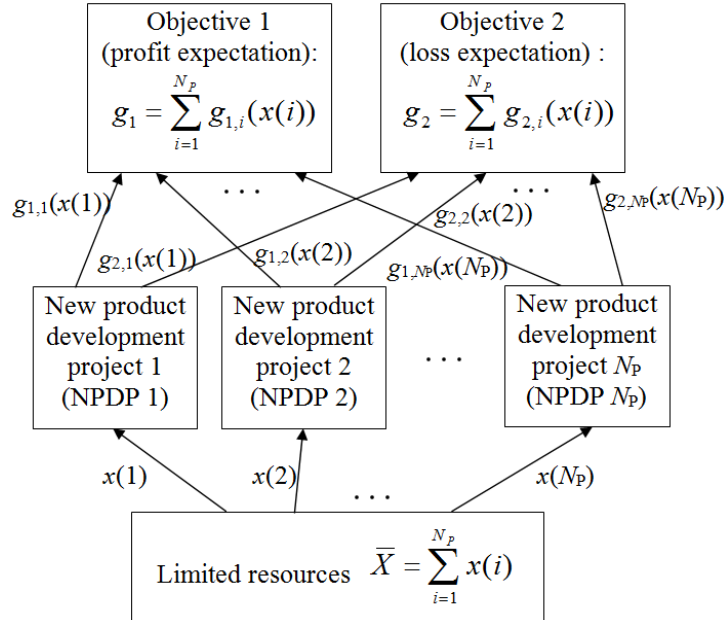


Fig.1. Illustration of MONPD

Suppose we have limited resources,  $\bar{X}$ , to support  $N_p$  NPDPs. Let  $x$  denote an allocation strategy, and  $0 \leq x(i) \leq \bar{X}$  denote the resources allocated to NPDP  $i$ , for  $i=1, \dots, N_p$ . With allocated resources  $x(i)$ , the profit expectation of NPDP  $i$  is  $g_{1,i}(x(i))$ , and the associated loss expectation is  $g_{2,i}(x(i))$ . Then for an allocation strategy  $x$ , the total profit expectation and loss expectation are

$$g_1 = \sum_{i=1}^{N_p} g_{1,i}(x(i)) , \tag{18}$$

$$g_2 = \sum_{i=1}^{N_P} g_{2,i}(x(i)) , \quad (19)$$

respectively. Then, with  $g_1$  and  $g_2$  as two objective functions, MONPD is formulated as

$$\max_x g_1 , \text{ and } \min_x g_2 \quad (20)$$

subject to (18), (19) and

$$\bar{X} = \sum_{i=1}^{N_P} x(i) . \quad (21)$$

The work in [31] is used to calculate complete Pareto front for discrete MOOPs. In this study, we assume there is a minimal investment unit  $\Delta x$  for resource allocation, and for any  $i=1,\dots,N_P$ , we have

$$x(i) = n(i)\Delta x , \quad (22)$$

where  $n(i) \geq 0$  is an integer. Suppose there are  $N_{TNIU}$  investment units in total, i.e.,

$$\bar{X} = N_{TNIU} \Delta x , \quad (23)$$

then we know for each  $i=1,\dots,N_P$ ,  $x(i)$  has  $(N_{TNIU}+1)$  choices, i.e.,  $x(i) \in \{0, \Delta x, \dots, N_{TNIU} \Delta x\}$ . With the minimal investment unit  $\Delta x$ , Constraint (21) is equivalent to

$$N_{TNIU} = \sum_{i=1}^{N_P} n(i) . \quad (24)$$

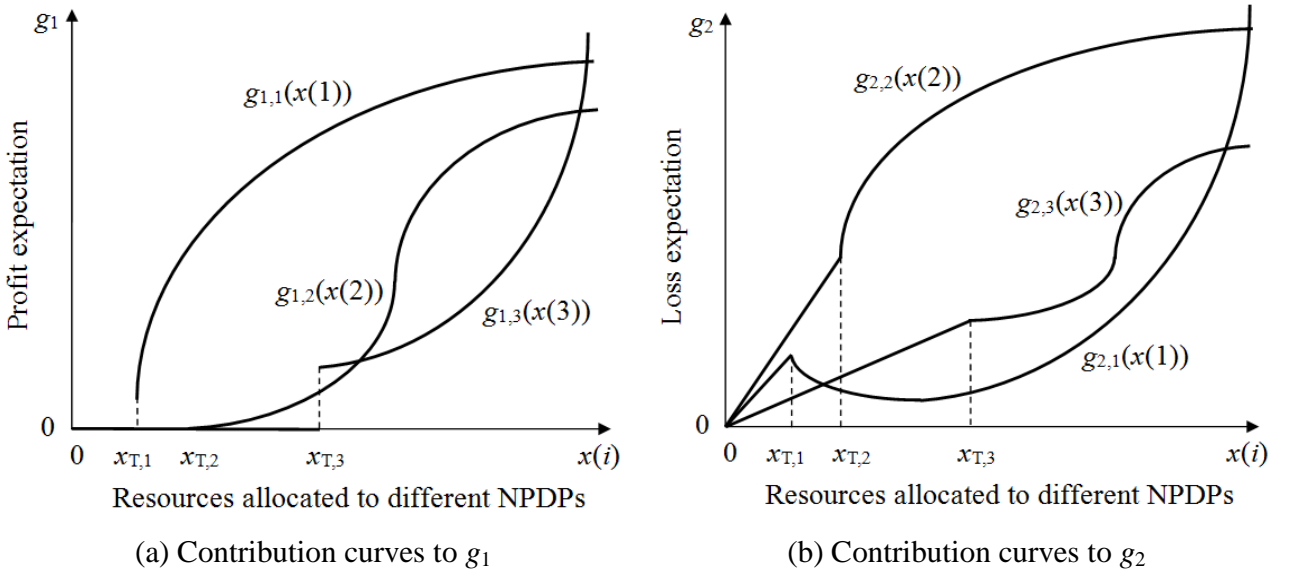


Fig.2. Illustration of contribution curves

The complexity of MONPD mainly comes from  $g_{j,i}(x(i))$ , which determines the contribution of NPDP

$i$  with allocated resources  $x(i)$  to objective function  $g_j$ ,  $i=1, \dots, N_P$ , and  $j=1, 2$ . Basically, a contribution curve is nonlinear, and the MONPD involves a combination of different shaped nonlinear contribution curves. The complexity is illustrated by the contribution curves in Fig.2, where there are 3 NPDPs, and therefore 6 contribution curves of different shapes, which are totally project-dependent. Regarding the profit expectation of NPDP  $i$ , there is usually a threshold  $x_{T,i}$ , and if the allocated resources to NPDP  $i$  is below the threshold, i.e.,  $x(i) \leq x_{T,i}$ , then the project has no way to succeed, and therefore will make no profit at all. Regarding the loss expectation of NPDP  $i$ , when  $x(i) \leq x_{T,i}$ , the loss often linearly increases as  $x(i)$  goes up, and the gradient largely depends on what percentage of  $x(i)$  is invested in reusable facilities.

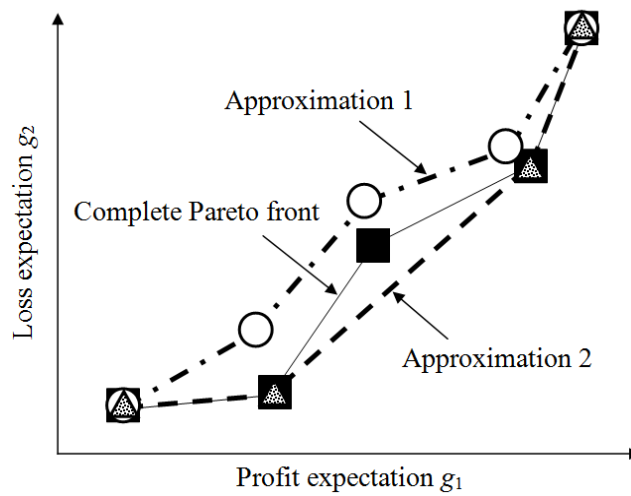


Fig.3. Complete Pareto front and approximations

For discrete MONPD, a typical complete Pareto front is given in Fig.3, which is composed of squares and solid lines. Since the MONPD needs to maximize  $g_1$  and minimize  $g_2$  simultaneously, the Pareto front is an increasing curve. It should be noted that the Pareto front of the ROP in [31] is a decreasing curve, because all objectives need to be minimized there. Therefore, as will be explained later in Section 4.2, the method design for MONPD is rather different from that for the ROP in [31]. Such an increasing curve in MONPD implies a large profit expectation always comes with a large loss expectation. Any point in the right-bottom side of the Pareto front is impossible to achieve. For any point in the left-top side of the Pareto front, the associated  $x$  is not Pareto optimal, which means there exists at least one solution leading to a larger profit expectation without increasing the loss expectation, or a smaller loss expectation without decreasing the profit expectation. Fig.3 also gives two approximations of the Pareto front and one is plotted by circles and dash-and-dot lines, and the other by triangles and dash lines. As illustrated in Fig.3, there is often a difference between the complete Pareto front and an approximation. The difference is

usually uncertain to decision makers, in other words, if an approximation of the Pareto front is provided, decision makers will have no idea whether there exists any other Pareto-optimal solution (e.g., in Fig.3, Approximation 2 misses out one Pareto point, which is probably the best tradeoff between two objectives), or even whether a provided solution associated with a point on the approximated Pareto front is really Pareto-optimal (e.g., in Fig.3, Approximation 1 actually has 3 false Pareto points). Therefore, using an approximation of Pareto front implies (i) some solutions most preferable by decision makers might be actually missed out, and (ii) arguments might occur in the decision making process because different decision makers could choose different approximation methods. Obviously, if we can calculate the complete Pareto front rather than approximating it, then decision makers will be free of the above issues. With the complete Pareto front at hand as illustrated in Fig.3, decision makers in MONPD can easily and accurately find an ideal resource allocation strategy according to, say, their risk-taking willingness and market uncertainties.

## **4 A RIPPLE-SPREADING ALGORITHM FOR MONPD**

### ***4.1 Basic idea of ripple-spreading algorithm (RSA)***

It is well known that many successful computational intelligence techniques are actually inspired by certain natural systems or phenomena [39]. For instance, genetic algorithms are inspired by natural selection and evolutionary processes, artificial neural networks by the animal brain, particle swarm optimization by the learning behavior within a population, and ant colony optimization by the foraging behavior of ants. Following the common practice of learning from nature in the computational intelligence domain, we have recently reported some ripple-spreading models and algorithms [40]-[44]. The hypothesis behind these is the following: the natural ripple-spreading phenomenon, as a pervasive phenomenon in the universe, reflects certain fundamental organization/optimization principles in nature, and such principles are to be found in many systems and problems around us. Taking such inspiration when developing models and algorithms to study such systems and problems, we are likely to better match/reflect the embedded principles of these systems, and therefore generate more effective solutions. For example, by mimicking the natural ripple-spreading phenomenon, we developed some useful models to study complex networks [40], air traffic management [41], and epidemic dynamics [42], and some effective algorithms to tackle ROPs [43], [44].

Basically, ripple-spreading algorithms (RSAs) achieve optimality by taking advantage of the optimization principle reflected in the natural ripple-spreading phenomenon, which is very simple: a ripple spreads out at the same speed in all directions, and therefore it reaches spatial points in order according to

their distance from the ripple epicenter, i.e., it always reaches the closest point first. Intuitively, one may get a feeling that this optimization principle could be used to find the closest interesting points (e.g., to find the closest gas station), or more generally, to find the shortest path. Therefore, we successfully developed some effective RSAs for ROPs in [43] and [44]. Most existing methods for ROPs are centralized, top-down, logic-based search algorithm. Differently, RSAs are actually decentralized, bottom-up, agent-based simulation model. By defining the behavior of individual nodes, optimality will automatically emerge as a result of the collective performance of the model. As illustrated in Fig.4, the first ripple starts from the source node, i.e., node 1; when a ripple reaches a directly connected but unvisited node, that new node will be activated to generate its own ripple; when all of those nodes that are directly connected to the epicenter node of a ripple are visited (not necessarily by the same ripple), that ripple will then stop and be eliminated; when the destination node, i.e., node 4, is visited for the first time, the first shortest route is then found [43]; the simulation keeps going on until the destination node is reached for the  $k^{\text{th}}$  time, then the  $k$  shortest routes are found in order [44]. The above process is likened to a ripple relay race, where ripples compete with each other to reach the destination node. During the entire process, all ripples always travel at the same preset constant speed.

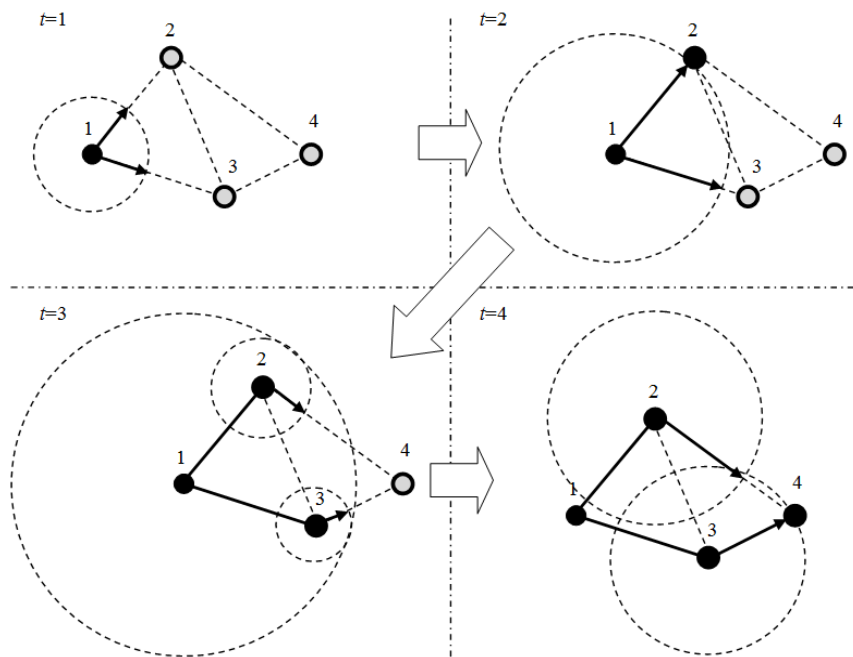


**Fig.4.** Illustration of RSA to find the shortest path

## 4.2 Bespoke RSA for MONPD

The most difficult part of the general methodology in Section 2.2 is to find/design a problem-specific algorithm to calculate the  $k$  best single-objective solutions to an MOOP. In this sub-section, we will design an RSA which is capable of calculating the  $k$  best solutions in terms of the profit expectation  $g_1$  and the loss expectation  $g_2$ , respectively.

As discussed in Section 4.1, the RSA in [44] can resolve the  $k$  shortest paths problem. To apply a RSA to the MONPD, we need to transform the MONPD into a special ROP. Please note that the ROP in [44] is a minimization problem, whilst optimizing profit expectation is a maximization problem. Therefore, we have to make some modifications before we can apply RSA to the MONPD.

To transform the MONPD into a ROP, we need to construct two directed route networks for the MONPD, one for  $g_1$  and the other for  $g_2$ . In the route network for  $g_j$ , firstly we set up a dummy source node. Then we add  $N_{\text{TNIU}}+1$  new nodes, representing different resource allocations to NPDP1. Then we establish directed links from the source to each of these  $N_{\text{TNIU}}+1$  nodes. In the route network for  $g_1$ , the length of the link which connects to the node of  $n\Delta x$  allocation to NPDP1 is set as

$$l_{n,1} = g_{1,1}(\bar{X}) - g_{1,1}(n\Delta x), n=0, \dots, N_{\text{TNIU}}, \quad (25)$$

and in the route network for  $g_2$ , the length is

$$l_{n,1} = g_{2,1}(n\Delta x), n=0, \dots, N_{\text{TNIU}}. \quad (26)$$

Assume we have added  $N_{\text{TNIU}}+1$  nodes associated with different resource allocations to NPDP  $i$ ,  $i < N_{\text{P}}-1$ . Then we add another  $N_{\text{TNIU}}+1$  new nodes, representing different resource allocations to NPDP  $i+1$ . Then we establish directed links from NPDP  $i$  nodes to NPDP  $i+1$  nodes subjected to Constraint (21) or (24). In the route network for  $g_1$ , the length of the link which connects to the node of  $n\Delta x$  allocation to NPDP  $i+1$  (i.e.,  $x(i+1)=n\Delta x$ ) is set as

$$l_{n,i+1} = g_{1,i+1}(\bar{X}) - g_{1,i+1}(n\Delta x), n=0, \dots, N_{\text{TNIU}}, \quad (27)$$

and in the route network for  $g_2$ , the length is

$$l_{n,i+1} = g_{2,i+1}(n\Delta x), n=0, \dots, N_{\text{TNIU}}. \quad (28)$$

After we have added  $N_{\text{TNIU}}+1$  nodes associated with different resource allocations to NPDP  $N_{\text{P}}-1$ , then we add a dummy destination node, and establish a directed link from every NPDP  $N_{\text{P}}-1$  node to the destination. As will be explained later, the length of a link connected to the destination, denoted as  $l_{n,N_{\text{P}}}$ , will be dynamically set up during the following ripple relay race. Fig.5 gives a simple illustration about how to construct a route network for MONPD, where  $N_{\text{P}}=4$  and  $N_{\text{TNIU}}=3$ .

With the constructed route network for  $g_j$ , we can develop a ripple relay race to calculate the  $k$  best solutions in terms of objective  $g_j$  for MONPD. Basically, the new race process is similar to that in [44], which aims to resolve the  $k$  shortest paths problem, and the major modifications are: (i) a new ripple at a node needs to select out feasible links from established links according to Constraint (21) or (24); (ii) the length  $l_{n,NP}$  needs to be dynamically reset according to the resource allocations of NPDP1 to NPDP  $N_P-1$ . Since a ripple-spreading algorithm is actually a bottom-up, agent-based simulation model we can easily define problem-specific node behavior to achieve the above two modifications. Therefore as a result of the above two modifications, the route network for  $g_j$  in MONPD can be viewed as a dynamic network rather than the static ones in [31], [43] and [44].

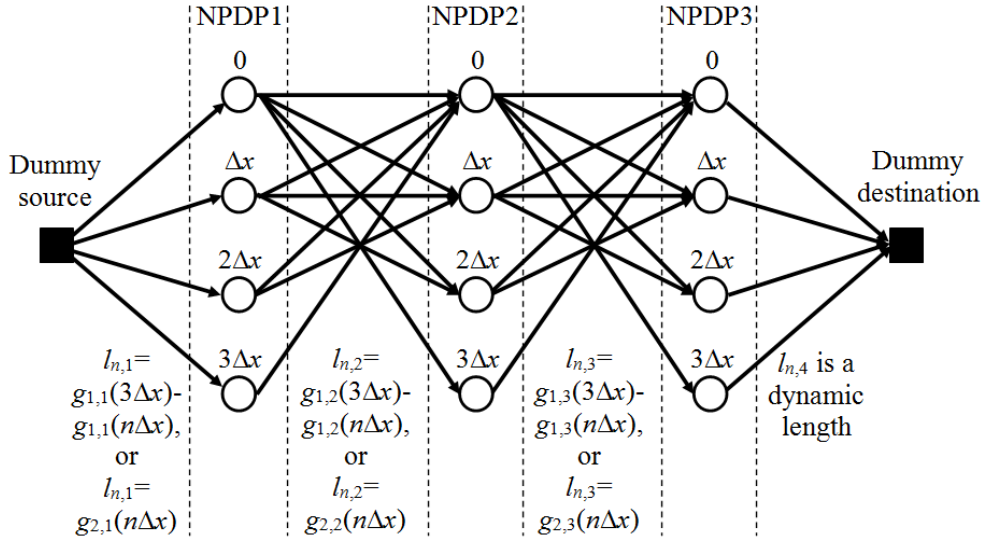


Fig.5 The construction of route network for  $g_j$  in MONPD

The following are the details of the new ripple relay race to calculate the  $k$  best solutions in terms of objective  $g_j$  for MONPD.

Step 1. Set the ripple spreading speed as  $s$ . Set time  $t=0$ . Let  $n_{\text{DNR}}=0$  denote how many times the dummy destination node has been reached by ripples. Start an initial ripple at the dummy source node. In the relay race, every ripple needs to record which existing ripple triggers it, and which node it originates. For the initial ripple at the dummy source node, it is triggered by no other existing ripple.

Step 2. If  $n_{\text{DNR}} < k$ , update  $t=t+1$ , and repeat the following process. For each existing ripple, increase its radius by  $s$ . Compare its radius with the length of every feasible link. As emphasize before, the route network of MONPD is a dynamic network. Although we have established a static network topology to run the ripple relay race, for a ripple originating from the NPDP  $i$  node of  $n(i)\Delta x$ ,  $i=2, \dots, N_P-2$ , not

all established links are feasible to travel on. Suppose a stimulating ripple passes the NPDP  $m$  node of  $n(m)\Delta x$ ,  $m=1, \dots, i-1$ , and then trigger a new ripple at the NPDP  $i$  node of  $n(i)\Delta x$ . Then, for this new ripple, an established link connected to the NPDP  $i+1$  node of  $n(i+1)\Delta x$  is feasible if

$$\bar{X} \geq \sum_{m=1}^{i+1} n(m)\Delta x. \quad (29)$$

The dynamic feature of the MONPD network also results from the length of a link from an NPDP  $N_p-1$  node to the dummy destination node, which depends on the so-far route along which the stimulating ripple of the current NPDP  $N_p-1$  ripple travels. Suppose the stimulating ripple passes the NPDP  $i$  node of  $n(i)\Delta x$ ,  $i=1, \dots, N_p-2$ , and the current NPDP  $N_p-1$  ripple originates from the NPDP  $N_p-1$  node of  $n(N_p-1)\Delta x$ , then in the route network for  $g_1$ , the link length from the NPDP  $N_p-1$  node of  $n(N_p-1)\Delta x$  to the dummy destination node is

$$l_{n, N_p} = g_{1, N_p}(\bar{X}) - g_{1, N_p}\left(\bar{X} - \sum_{i=1}^{N_p-1} n(i)\Delta x\right), \quad (30)$$

and in the route network for  $g_2$ , the link length is

$$l_{n, N_p} = g_{2, N_p}\left(\bar{X} - \sum_{i=1}^{N_p-1} n(i)\Delta x\right). \quad (31)$$

If the radius is larger than a feasible link,

Step 2.1. If the end node of the feasible link is not the dummy destination node, then a new ripple will be triggered at the end node of the feasible link, and the initial radius of the new ripple is the radius of the stimulating ripple minus the length of the feasible link.

Step 2.2. If the end node of the feasible link is the dummy destination node, then update  $n_{\text{DNR}} = n_{\text{DNR}} + 1$ . Track back the current ripple to reveal the  $(n_{\text{DNR}})$ th best solution in terms of objective  $g_j$ . If  $n_{\text{DNR}} = k$ , go to Step 3.

Step 3. Stop the ripple relay race, and output the  $k$  best solutions in terms of objective  $g_j$ .

It is easy to derive that the  $k^{\text{th}}$  shortest path in the constructed route network for  $g_j$  is associated with the  $k^{\text{th}}$  best solution in terms of optimizing the value of  $g_j$  (i.e., maximizing  $g_1$  or minimizing  $g_2$ ). With the above ripple-spreading algorithm, the methodology in Section 2.2 becomes practicable for MONPD. One may argue that, for the sake of computational efficiency, the methodology in Section 2.2 demands an algorithm to calculate the  $k^{\text{th}}$  best single-objective solution rather than the  $k$  best single-objective solutions. This is not a problem at all. When integrating the above ripple-spreading algorithm into the methodology in Section 2.2, the ripple relay race will be initialized once and only once. Every time when the dummy

destination node is reached by a ripple, the race process will be paused or frozen. Then the newly found best solution will be checked with all previously found best solutions, to see if the complete Pareto front is covered. If not, then the race process will be resumed to find the next best solution.

The optimization of profit expectation  $g_1$  defined in (20) is a maximization problem, to which the RSA in [26, [43] and [44] cannot apply directly. The setup of link length according to (25), (27) and (30) in the route network for  $g_1$  actually converts the original maximization of  $g_1$  into a minimization problem. This design enables the calculation of the  $k^{\text{th}}$  largest profit expectation by the RSA. Similar to approaches in [43] and [44], one may derive that the optimality of the RSA reported in this section is guaranteed by the optimization principle reflected in the natural ripple-spreading phenomenon. In other words, the reported RSA can theoretically guarantee the finding of the  $k^{\text{th}}$  best single-objective solution for MONPD. Therefore, applying the general methodology in Section 2.2 to calculate the complete Pareto front of MONPD becomes practically possible.

## 5 SIMULATION RESULTS

In this section, we present some simulation results to demonstrate the practicability and effectiveness of the proposed method to calculate the complete Pareto front for MONPD. There are three parts of simulation results: (i) comparative results with a brute-force search (BFS) method to prove the discovery of the complete Pareto front; (ii) comparative results with an aggregate objective function (AOF) based method and a Pareto-compliant ranking (PCR) based method to show the advantage of new method; (iii) analyses based on the complete Pareto front to illustrate the usefulness of the new method. In the simulation, the total budget  $\bar{X}$  has 9 options: [10 15 20 25 30 35 40 45 50] (million money unit), which represent 8 scenarios. Resources need to be allocated to five different NPDPs, whose profit expectations and loss expectations are given in Fig.6. Basically, the profit expectations all go up as the allocated resources increase. For NPDP1 to NPDP4 (e.g., traditional categories of products such as clothes, toys and food), the profit expectation will approach a certain upper bound gradually, while for NPDP5 (e.g., high-tech products such as online games), the profit expectation rises exponentially. Both expectation curves of NPDP3 are piece-wise, and this is usually related to contracted order of customized product. In other words, a new product is especially developed according to the order of a certain customer, and once developed successfully, will be sold for sure (therefore the loss expectation may become zero once the basic order is fulfilled), but only to that customer. Further development may be carried out beyond the basic order, but the customer is not contracted to buy or pay a higher price. Therefore, the loss expectation goes up from zero again. NPDP2 is a more generalized case of NPDP3.

In the comparison with BFS, the minimal investment unit  $\Delta x$  is set as 1 million, so that the simulation results can be better plotted to demonstrate the advantage of new method. Some results are given in Table 1 and Fig.7, where  $N_{NS}$  is total number of solutions explored by a method,  $N_{PPF}$  is number of Pareto points found by a method,  $N_{SS}$  is the total number of solutions in the solution space, and  $N_{NS}/N_{SS}$  indicates the search efficiency of a method. Firstly, the simulation results confirm that the Pareto fronts identified by the new method are exactly the same as those found by the BFS. Table 1 shows that the Pareto fronts found by the new method have exactly the same number of Pareto points as those by the BFS. From Table 1, one can also see the new method has a much better search efficiency than the BFS, and in general, the advantage becomes more significant as the problem complexity increases (i.e., when  $\bar{X}$  goes up). Fig.7 gives four examples to illustrate why the new method is much more computationally efficient. According to the theories in [31], the solutions explored by the new method are only those pink star points (including all Pareto point plotted as red circles), which are below or on the right-hand side of the yellow dash lines in Fig.7. Those yellow dash lines are drawn according to the  $k^{\text{th}}$  best solutions which trigger the termination criteria of the new method, i.e., Conditions (16) and (17) in Section2.2. For example, in the case of Fig.7(c), the 7<sup>th</sup> best solution in terms of  $g_1$  and the 6<sup>th</sup> best solution in terms of  $g_2$  satisfy the Conditions (16) and (17). Because of the ripple-spreading nature when searching for the  $k^{\text{th}}$  best single-objective solution, the new method simply stops before any more solution is explored. Those green star points in Fig.7 are all solutions which are not explored by the new method. When comparing those green star points and those pink ones, one may get an intuitive feeling how computationally efficient the new method could be against the BFS.

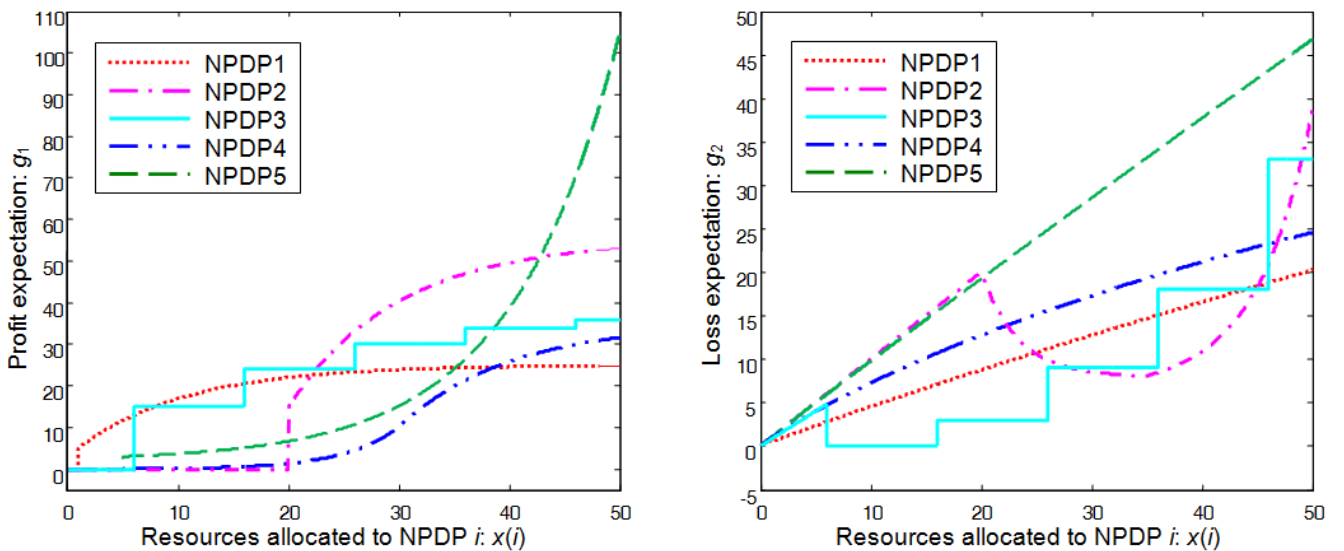


Fig.6 Contribution curves used in the simulation

Table 1 Comparative results between BFS and the new method ( $\Delta x$  is set as 1 million)

|            |                 | $\bar{X}=10m$ | $\bar{X}=15m$ | $\bar{X}=20m$ | $\bar{X}=25m$ | $\bar{X}=30m$ | $\bar{X}=35m$ | $\bar{X}=40m$ | $\bar{X}=45m$ | $\bar{X}=50m$ |
|------------|-----------------|---------------|---------------|---------------|---------------|---------------|---------------|---------------|---------------|---------------|
| BFS        | $N_{NS}$        | 1001          | 3876          | 10626         | 23751         | 46376         | 82251         | 135751        | 211876        | 316251        |
|            | $N_{PPF}$       | 5             | 10            | 9             | 10            | 13            | 7             | 5             | 12            | 29            |
|            | $N_{NS}/N_{SS}$ | 1             | 1             | 1             | 1             | 1             | 1             | 1             | 1             | 1             |
| New method | $N_{NS}$        | 12            | 62            | 122           | 83            | 198           | 34            | 12            | 66            | 306           |
|            | $N_{PPF}$       | 5             | 10            | 9             | 10            | 13            | 7             | 5             | 12            | 29            |
|            | $N_{NS}/N_{SS}$ | 0.0120        | 0.0160        | 0.0115        | 0.0035        | 0.0043        | 0.0004        | 0.0001        | 0.0003        | 0.001         |

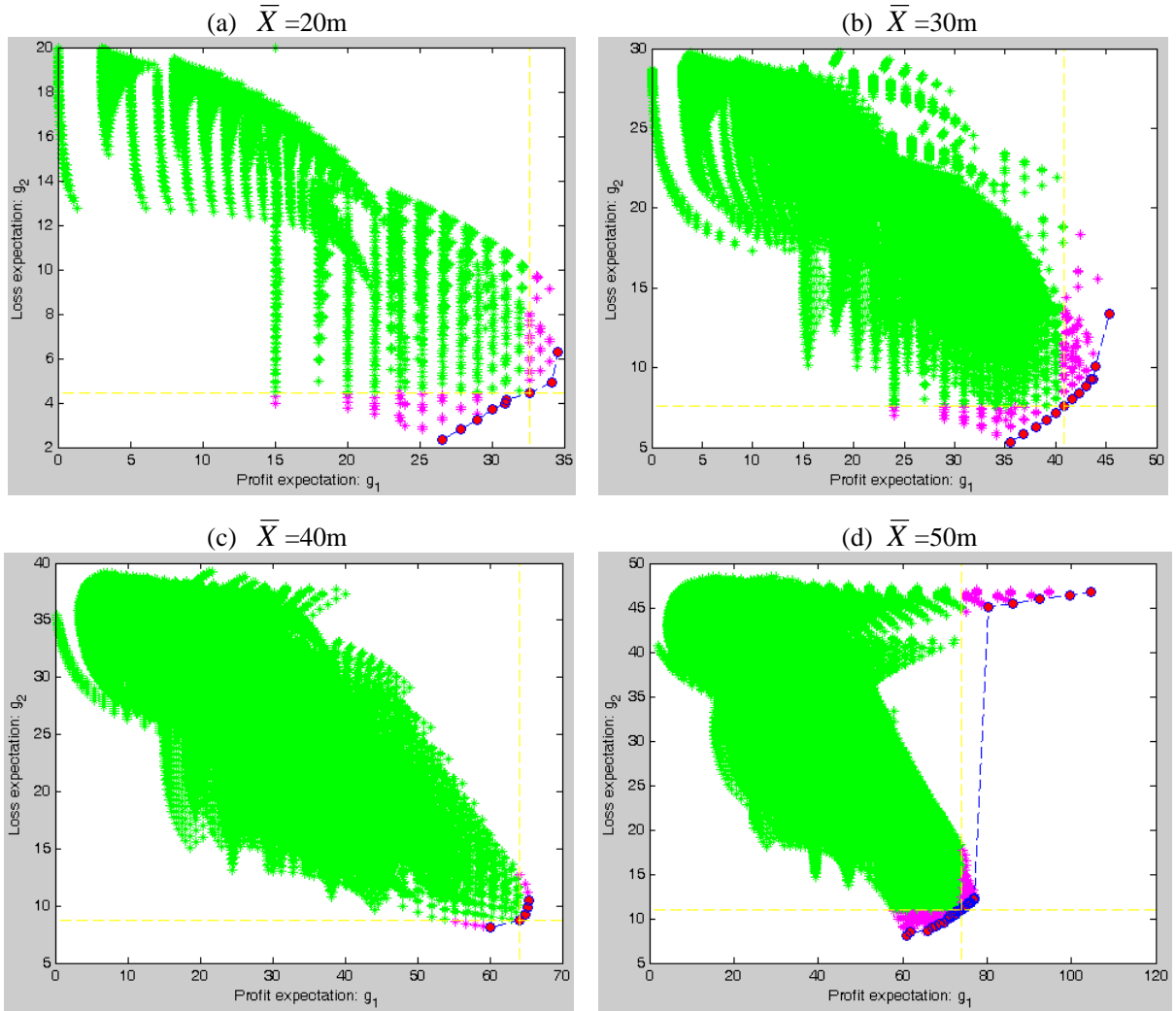


Fig.7 Completeness of the calculated Pareto fronts ( $\Delta x$  is set as 1 million)

Now, we compare the new method with two of the most popular MOOP methods: one is an AOF method, and the other is a well known PCR method, i.e., the NSGA-II in [19]. This time, we increase the problem complexity by setting  $\Delta x=0.2$  million. In the AOF method, in a similar fashion to traditional



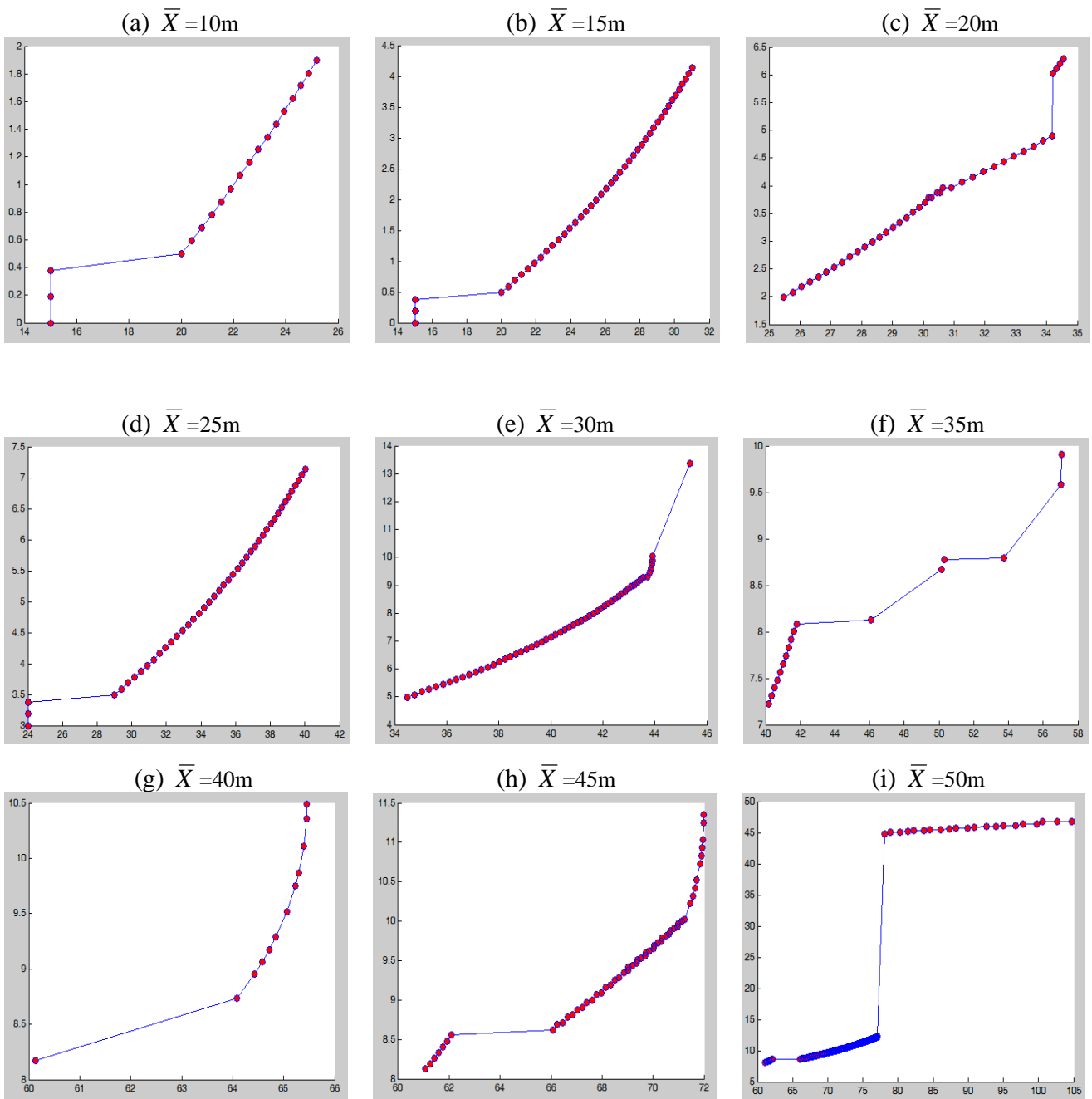


Fig.8 Calculated Pareto fronts in different scenarios of MONPD

(x axis is  $g_1$ , and y axis is  $g_2$ ;  $\Delta x$  is set as 0.2 million)

Finally, we will show what good things a complete Pareto front may do for decision makers in MONPD. One reason for why AOF methods are widely accepted in the practice of MOOP is because decision makers have to make only one single choice anyway. Once decision makers can agree on and provide a set of weights, AOF methods will output a unique Pareto optimal solution as the final choice. Given a set of weights, a complete Pareto front can no doubt also help decision makers with making the same single

choice. In the case of MONPD, decision makers just need to provide a coefficient  $\alpha$  to indicate how much loss risk ( $g_2$ ) they are willing to take to get a unit profit expectation ( $g_1$ ). Then in the objective space, we move a straight-line with  $\alpha$  as the gradient, from the right-bottom towards the left-top, until it touches the Pareto front, and the point of tangency gives the ideal choice to decision makers. Although AOF methods can also find such an ideal choice given the value of  $\alpha$ , the new method offers much more detail to decision makers. In particular, a complete Pareto front provides the most comprehensive support to backup solutions. Fig.9 gives some examples in the MONPD scenario of  $\bar{X}=40m$  and  $\Delta x=0.2m$ . Basically, a gambling manager may go with the Pareto point at the right top (e.g., s/he is willing to take a risk of 16.2 units of loss for one unit profit). A cautious manager can choose the Pareto point at the left bottom (e.g., even a risk of 0.1 units of loss seems too much). A reasonable manager willing to take a risk of 0.89 units of loss for one unit profit can choose the green Pareto point. Although the AOF method can do the same thing once  $\alpha$  is specified, it cannot provide sufficient backup solutions. For example, from Fig.9, one can see that, once the complete Pareto front is available, then for the gambling manager willing to take a risk of 16.2 units loss for one unit profit, s/he may actually choose the second right top Pareto point, which offers almost the same profit expectation but with an obviously smaller loss expectation. This is a significantly beneficial thing offered by the new method.

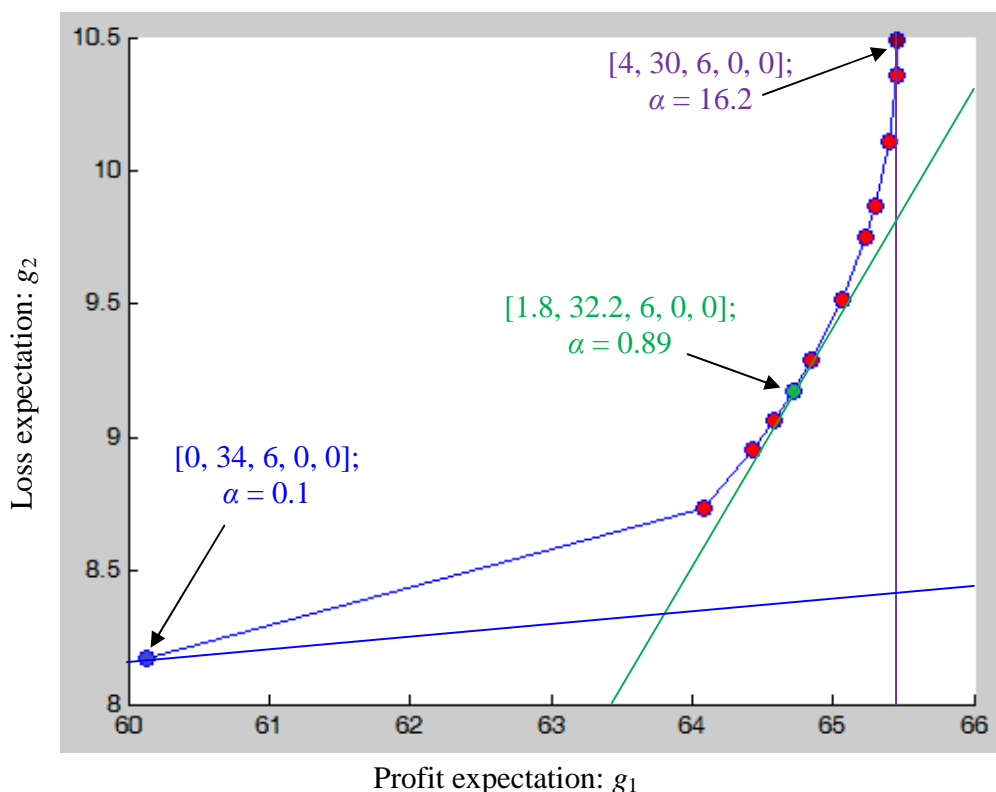


Fig.9 Using complete Pareto front to help with single-choice making ( $\bar{X}=40m$  and  $\Delta x=0.2m$ )

As mentioned in Section 1, AOF methods are often criticized for their elements of subjectivity as they demand weights from decision makers. For the new method, the coefficient  $\alpha$  largely relied on the risk attitudes of the decision makers and their understanding of the current and future market environments. No doubt there are significant uncertainties and no decision makers can be 100% sure about the value of  $\alpha$  they provide. A complete Pareto front can minimize the influence of such uncertainties. With a complete Pareto front at hand, we can easily and accurately work out for what range of  $\alpha$  value each individual Pareto point may serve as the ideal choice for decision makers. Fig.10 gives an illustration in the MONPD scenario of  $\bar{X}=20m$  and  $\Delta x=0.2m$ . If we invest 8.6m and 11.4m in NPDP1 and NPDP3, and nothing in NPDP2, NPDP4 and NPDP5, respectively (the associated Pareto point is plotted as a solid green circle), respectively, then the complete Pareto front tells that, for any  $0.34 \leq \alpha \leq 3.79$  (because of uncertainties in risk taking willingness and market environment), the solution is still the ideal choice. The capability of accurately assessing to what extent a solution may serve as the ideal choice is no doubt highly useful to decision makers in MONPD. This is another good thing the new method can do beyond the existing methods. Obviously the new and advantageous decision-making analyses demonstrated by Fig.9 and Fig.10 are firmly rooted in the capability of calculating complete Pareto front. This apparently verifies the importance of the methodology described in Section 2.

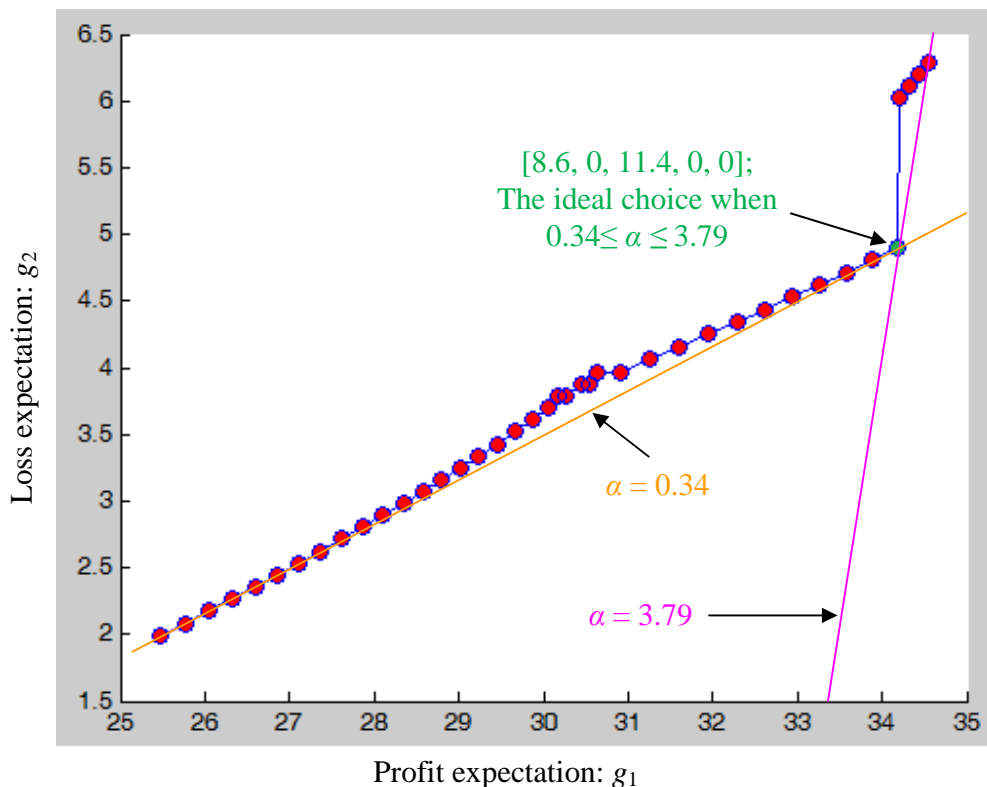


Fig.10 The extent to which a Pareto-optimal solution serves as the ideal choice ( $\bar{X}=20\text{m}$  and  $\Delta x=0.2\text{m}$ )

## 6 CONCLUSIONS AND FUTURE WORK

Profit expectation and loss expectation are two concerns of decision makers in front of several new product development (NPD) projects. The decision of how to allocate limited resources among projects in order to maximize the profit expectation and minimize the loss expectation (a challenging task) falls in the scope of a multi-objective optimization problem (MOOP). As a key concept in the study of MOOPs, the Pareto front can theoretically provide the best support to decision makers, but unfortunately, there is often a lack of practical methods to find the complete Pareto front, and most existing methods only give an approximation to it. Based on our previous theoretical work, this paper develops a practicable method to calculate the complete Pareto front for multi-objective new product development (MONPD). Some new theoretical results are reported to guarantee optimality, and then a ripple-spreading algorithm for calculating the  $k^{\text{th}}$  best single-objective solution is developed to deliver practicability. The simulation results clearly show that finding the complete Pareto front can provide the best support to decision makers of MONPD, because, for example, it enables decision makers to conduct many new useful analyses which are basically impossible based on an approximation of Pareto front.

It should be emphasized that the design of algorithm for calculating the  $k^{\text{th}}$  best single-objective solution is highly problem-dependent and often not an easy task, so, the general applicability and tractability of the theoretical methodology adopted demands further sustained effort to be reinforced in future study. In particular, more comparisons need to be conducted not only for benchmark MOOPs which already have many mature methods to calculate Pareto front, but also for those newly emerging MOOPs which lack effective methods to resolve them. Only in this way can the potential of the reported methodology be fully explored.

## REFERENCES

- [1] K.T. Ulrich, S.D. Eppinger, *Product Design and Development*, 3rd Edition, McGraw-Hill, New York, 2004.
- [2] D.C. Musso, E. Rebentisch, N. Gupta, *The Path to Developing Successful New Products*, MIT Sloan Management Review Press, 2009.
- [3] B.T. Barkley, *Project Management in New Product Development*, McGraw-Hill, 2007.
- [4] J. Kim, D. Wilemon, Sources and assessment of complexity in NPD projects, *R&D Management* 33 (1) (2007) 16-30.

- [5] A. Khurana, S.R. Rosenthal, Towards Holistic "Front Ends" in New Product Development, *Journal of Product Innovation Management* 15 (1) (1998) 57–75.
- [6] H.M. Markowitz, Portfolio Selection, *The Journal of Finance* 7 (1) (1952) 77–91.
- [7] N. Barr, *Economics of the welfare state*, New York, Oxford University Press, USA, 2004.
- [8] R.E. Steuer, *Multiple Criteria Optimization: Theory, Computations, and Application*, New York: John Wiley & Sons, Inc. ISBN 047188846X, 1986.
- [9] Y. Sawaragi, H. Nakayama, T. Tanino, *Theory of Multiobjective Optimization (vol. 176 of Mathematics in Science and Engineering)*, Orlando, FL: Academic Press Inc. ISBN 0126203709, 1985.
- [10] I. Das, J.E. Dennis, Normal-Boundary Intersection: A New Method for Generating the Pareto Surface in Nonlinear Multicriteria Optimization Problems, *SIAM Journal on Optimization* 8 (1998) 631–657.
- [11] I. Das, J.E. Dennis, Normal-Boundary Intersection: An Alternate Method For Generating Pareto Optimal Points In Multicriteria Optimization Problems, NASA Contractor Report 201616, ICASE Report No. 96-62, 1996.
- [12] A. Messac, A. Ismail-Yahaya, C.A. Mattson, The normalized normal constraint method for generating the Pareto front, *Structural and multidisciplinary optimization* 25(2) (2003) 86–98.
- [13] A. Messac and C. A. Mattson, Normal constraint method with guarantee of even representation of complete Pareto front, *AIAA journal*, 42(10) (2004) 2101–2111.
- [14] T. Erfani, S.V. Utyuzhnikov, Directed Search Domain: A Method for Even Generation of Pareto Front in Multiobjective Optimization, *Journal of Engineering Optimization*, 12 (2010) 1–18.
- [15] A. Konak, D.W. Coit, A.E. Smith, Multi-objective optimization using genetic algorithms: A tutorial, *Reliability Engineering and System Safety* 91 (2006) 992–1007.
- [16] D.F. Jones, S.K. Mirrazavi, M. Tamiz, Multiobjective meta-heuristics: an overview of the current state-of-the-art, *Eur J Oper Res* 137(1) (2002) 1–9.
- [17] N. Srinivas, K. Deb, Multiobjective optimization using nondominated sorting in genetic algorithms. *Evol Comput* 2(3) (1994), 21–48.
- [18] J.D. Knowles, D.W. Corne, Approximating the nondominated front using the Pareto archived evolution strategy, *Evol Comput* 8(2) (2000) 149–72.
- [19] K. Deb, *Multi-objective optimization using evolutionary algorithms*, Wiley, New York, 2001.
- [20] D.A. Van Veldhuizen, G.B. Lamont, Multiobjective evolutionary algorithms: analyzing the state-of-the-art, *Evol Comput* 8(2) (2000) 125–47.
- [21] C. Horoba, Exploring the Runtime of an Evolutionary Algorithm for the Multi-Objective Shortest Path Problem, *Evol Comput* 18(3) (2010) 357-381.

- [22] D. Hadka, P. Reed, Borg: An Auto-Adaptive Many-Objective Evolutionary Computing Framework, *Evol Comput* 21(2) (2013) 231-259.
- [23] S.M. Venske, R.A. Gonçalves, M.R. Delgado, ADEMO/D: Multiobjective optimization by an adaptive differential evolution algorithm, *Neurocomputing* 127 (2014) 65-77.
- [24] A. Britto, A. Pozo, Using reference points to update the archive of MOPSO algorithms in Many-Objective Optimization, *Neurocomputing* 127 (2014) 78-87.
- [25] Y. Mei, K. Tang, X. Yao, Decomposition-Based Memetic Algorithm for Multiobjective Capacitated Arc Routing Problem, *IEEE Transactions on Evolutionary Computation* 15(2) (2011) 151-165.
- [26] J. Figueira, S. Greco, Multiple criteria decision analysis: state of the art surveys, Matthias Ehrgott, 2005.
- [27] D. Craft, T. Halabi, H. Shih, T. Bortfeld, Approximating convex Pareto surfaces in multiobjective radiotherapy planning, *Medical Physics* 33(9) (2006) 3399–3407.
- [28] R.T. Marler, J.S. Arora, Survey of multi-objective optimization methods for engineering, *Struct Multidisc Optim* 26 (2004) 369-395.
- [29] Y.Y. Haimes, L.S. Lasdon, D.A. Wismer, On a bicriterion formulation of the problems of integrated system identification and system optimization, *IEEE Trans. Syst. Man Cybern* 1 (1971) 296–297.
- [30] W. Stadler, J.P. Dauer, Multicriteria optimization in engineering: a tutorial and survey. In: Kamat, M.P. (ed.) *Structural Optimization: Status and Promise*, Washington, DC: American Institute of Aeronautics and Astronautics, 1992, pp.211–249.
- [31] X.B. Hu, M. Wang, E. Di Paolo, Calculating Complete and Exact Pareto Front for Multi-Objective Optimization: A New Deterministic Approach for Discrete Problems, *IEEE Transactions on Systems, Man and Cybernetics, Part B* 43(3) (2013) 1088-1101.
- [32] H.M. Markowitz, *Portfolio Selection: Efficient Diversification of Investments*, New York: John Wiley & Sons, 1959.
- [33] R. Merton, An analytic derivation of the efficient portfolio frontier, *Journal of Financial and Quantitative Analysis* 7 (1972) 1851-1872.
- [34] F. Black, R. Litterman, Global Portfolio Optimization, *Financial Analysts Journal*, 48 (1992) 28-43.
- [35] G. Debreu, The Coefficient of Resource Utilization, *Econometrica* 19 (1951), 273-292.
- [36] A. Nagurney, *Innovations in Financial and Economic Networks*, Edward Elgar Publishing, Cheltenham, England, 2003.
- [37] F. Castro, J. Gago, I. Hartillo, J. Puerto, J.M. Ucha, An algebraic approach to integer portfolio problems, *European Journal of Operational Research* 210(3) (2011) 647-659.

- [38] Z.C. Zhang, F. Chau, L. Xie, Strategic Asset Allocation for Central Bank's Management of Foreign Reserves: A new approach, MPRA Paper 43654, University Library of Munich, Germany, 2012.
- [39] S. Russell, P. Norvig, *Artificial Intelligence: A Modern Approach* (3rd ed.), Prentice Hall, 2010.
- [40] X.B. Hu, M. Wang, M.S. Leeson, E.L. Hines and E. Di Paolo, Deterministic Ripple-Spreading Model for Complex Networks, *Physical Review (E)* 83(4) (2011) Article ID 046123, 14 pages.
- [41] X.B. Hu, E. Di Paolo, A Ripple-Spreading Genetic Algorithm for the Aircraft Sequencing Problem, *Evolutionary Computation* 19(1) (2011) 77–106.
- [42] J.Q. Liao, X.B. Hu, M. Wang, and M.S. Leeson, Epidemic Modelling by Ripple-Spreading Network and Genetic Algorithm, *Mathematical Problems in Engineering* 2013 (2013) Article ID 506240, 11 pages.
- [43] X.B. Hu, Q. Sun, M. Wang, M.S. Leeson, and E. Di Paolo, A Ripple-Spreading Algorithm for Route Optimization, in: *2013 IEEE Symposium Series on Computational Intelligence*, 16-19 April 2013, Singapore.
- [44] X.B. Hu, M. Wang, D. Hu, M.S. Leeson, E.L. Hines, and E. Di Paolo, A Ripple-Spreading Algorithm for the  $k$  Shortest Paths Problem, in: *2012 the 3rd Global Congress on Intelligent Systems*, 6-8 Nov 2012, Wuhan, China.